FAST SETTLING MILLIMETRE-SCALE FIVE-HOLE PROBES

S.D. Grimshaw, J.V. Taylor
Whittle Laboratory
University of Cambridge
1 JJ Thomson Avenue
Cambridge, CB3 0DY, UK
Email: sdg33@cam.ac.uk

ABSTRACT

This paper investigates how the external geometry of a five-hole probe affects its accuracy and how internal geometry affects its settling time. An analytical model, which predicts settling time, is used to design an accurate, fast-settling, millimetre-scale probe. The paper has three components:

First, results are presented from a series of area traverses performed with five-hole probes which range in head diameter from 0.99 to 2.67 mm. It is found that the smallest probe gives the greatest accuracy when traversing the shear layers in blade wakes. However, it takes 3.4 times longer to complete this traverse than compared to the largest probe. This is because traverses with small probes require more time to allow the pressure readings to settle between each traverse position.
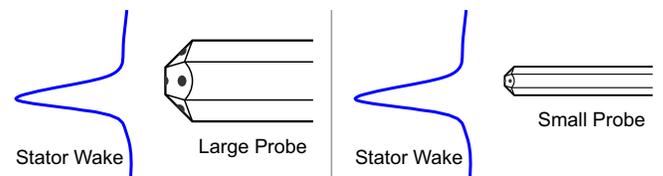
Second, an analytical model is developed which predicts settling time based upon the internal geometry of the probe. The adopted approach is capable of modelling any number of connected tubes with different lengths and diameters. It is validated against experimental measurements and is shown to give good agreement. This model can be used to ensure that probes are designed with acceptable settling times.

Finally, the analytical model is used to design an optimised five hole probe. Use of the model highlights two important results which are required to reduce settling time: First, the length of the smallest diameter tubes, i.e. the ones in the probe head, should be minimised. Second, the volume of tubing downstream of the head should be minimised. Applying these principles to a new probe design cuts the total traverse time by 71%, while maintaining the highest value of accuracy.

INTRODUCTION

Five-hole probes should have small outer dimensions to achieve high accuracy when measuring flowfields with steep spatial variation, such as those found in turbomachinery. This is demonstrated in Fig. 1(a): if the variation in the stagnation pressure field is of the same order as the distance between the probe holes, then the holes "see" different parts of the wake. The basis on which the calibration map of the probe was constructed, namely that stagnation pressure in the calibration jet is uniform, breaks down and the flow is measured incorrectly. Reducing probe head diameter reduces this effect and

a) Large five-hole probes have poor accuracy

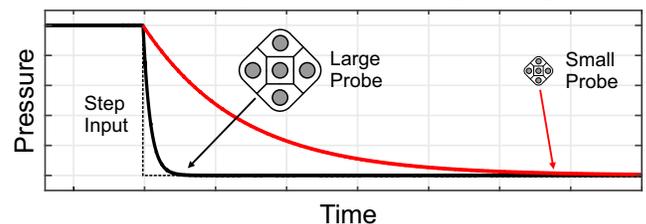b) Small five-hole probes have a long settling time

FIGURE 1: Trade between accuracy and traverse time in five-hole probe design

therefore improves the accuracy of the measurements.

Settling time is defined as the time taken for an output response to match a step change in pressure, as shown in Fig. 1(b). The step change is caused by the movement of the five-hole probe between traverse points and the response is the pressure measured at the end of the tubes connecting the probe head to the transducers. The settling time is sensitive to the internal geometry of this tubing; reducing probe head size requires tubes with smaller diameters and this results in longer settling times as illustrated in Fig. 1(b).

The aims of this paper are to first present the trade-off between probe head size, accuracy and settling time, and second, to develop an easy to implement, validated model which turbomachinery researchers can use to design fast-settling (<0.5 s) probes.

LITERATURE REVIEW
Area Traverses

Area traverses can be time consuming: Ligrani et al. [1] report an area traverse which takes 8 hours using a five-hole probe with head diameter of 1.22mm. Researchers faced with long traverse times

have a number of compromises available: tolerate long experiments, use fewer points and accept reduced resolution, or use larger probes which have shorter settling times but reduced spatial accuracy. Some progress can be made by clustering the traverse grid on features of interest, such as the method described by Lenherr et al. [2]. However, in the case of large experimental programmes the trade-off between time required and accuracy is likely to be encountered.

In the last 20 years much progress has been made in the design and use of unsteady probes for measuring time-varying pressures to bandwidths up to 100 kHz. Thorough reviews of this technology are presented by Sieverding et al. [3] and Ainsworth et al. [4]. In summary, unsteady probes achieve high frequency response by flush mounting fast response pressure transducers in the probe head. However, these type of probes are less robust than five-hole probes as the pressure transducers are more likely to be damaged and can be affected by temperature changes in the flow [4]. They are also significantly more expensive to fabricate or buy and require more effort to calibrate, operate and analyse. For these reasons unsteady probes are only used when time-accurate flow features need to be resolved. They are not used to speed up typical steady flow traverse measurements.

Returning, therefore, to five-hole probes; work by Naughton et al. [5] and Georgiou and Milidonis [6], to design, fabricate, calibrate and operate mm-scale probes with fast response times, is considered. In both cases the length of tube between the probe head and pressure transducer is minimised to reduce settling time and hence cut down traverse times. While these papers provide examples of fast-settling mm-scale probes they do not include analytical treatments of the settling time and instead rely on experimental tests, after the probes are fabricated, to confirm short response times. There is also no comparison of different probe designs, either in terms of accuracy or settling time.

Modelling flow in tubes

Flow in tubes has been studied extensively, beginning with Rayleigh, Helmholtz and Kelvin who first studied steady pipe flows towards the end of the 19th century. Since then, hundreds of studies have considered how to model the frequency or step response of pressure-sensing systems, where a pressure disturbance is transmitted to a transducer through a tube. The approaches reported can be split into three general groups as described by Stecki and Davis. [7]: numerical or analytical approximations of the full solutions, distributed parameter models and lumped parameter models.

The aim of this paper is to provide a simple, accurate model which can be used to predict settling time for steady flow measurements. A lumped parameter model is best suited for this as it is straightforward to implement, capable of predicting settling times for five-hole probes and provides useful physical insight. The classical second-order tube and cavity system is described by Delio [8] and Iberall [9] and the well-known electric circuit analogy for this system by Taback [10].

Modelling a five-hole probe with Delio or Taback's method assumes that the tube geometry is that of the hypodermic tubes in the probe head and the cavity volume is that of the connecting tubes and pressure transducer internal volume. It is not clear, therefore, how step-ups between tube diameters, e.g. from hypodermic tube to plastic tube, should be accounted for. An approach which addresses this issue was developed by Bergh and Tijdeman [11] and is further
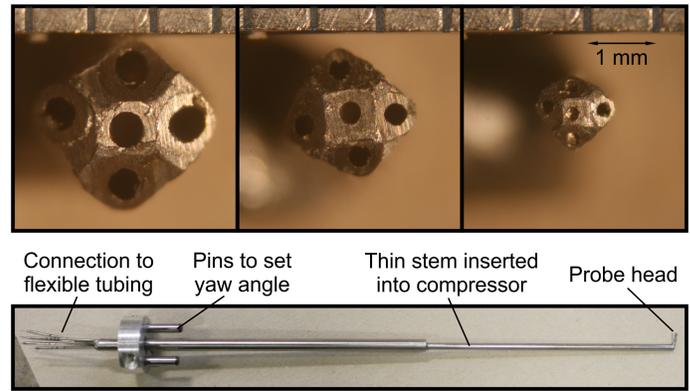

FIGURE 2: Top: Microscope view of probe head geometry. Bottom: Overview of probe design

described by Gumley [12] and Holmes [13]. This widely referenced work uses a recursive formula for the frequency response of any number of connected tubes and cavities. The method is recognised for its accuracy, however, despite being a lumped parameter model it is "[mathematically] complex, difficult to program and inherently linked to the frequency domain" [14].

For the researcher designing a mm-scale five-hole probe, an easy to implement time-domain approach, which can model step-ups in tube diameter, is required. The approach described in this paper builds on the electric circuit analogy but is able to model step-ups in probe diameter by recursively adding electrical components to Taback's second-order system. The model is shown to provide an accurate prediction of settling time for tubes representative of those typically used in the fabrication of five-hole probes.

1   MEASUREMENT ACCURACY OF PROBES

Errors are caused in the measurement of steeply varying flow fields if the head diameter of the five-hole probe is larger than the length-scale of the variation. In this section the origin of these errors is investigated. Traverses of a compressor stator wake are undertaken with five-hole probes of three different sizes and the results are examined with a new method for quantifying errors. The second part of the section presents the time taken to complete various processes during area traverses. This demonstrates that settling time is the most time-consuming activity when using the smallest probe.

Five-hole Probes

Three five-hole probes of different size are used to investigate the trade between traverse time and accuracy. They are constructed in a bundle of five stainless steel hypodermic tubes soldered together into a "plus" shape. The side holes are then ground to an angle of 45°. This gives a good balance between static pressure and flow angle sensitivity as discussed by Dominy and Hodson [15]. Photographs of the head geometries and the overall layout of the probes are shown in Fig. 2. Their dimensions are described in Table 1.

Probe Calibration

The probes are calibrated in a free jet, generated in a pull-down wind tunnel. The probes are moved over a range of $\pm 30°$ in yaw

TABLE 1: Five-hole probe dimensions. All dimensions in mm

Head diameter	D	2.67	1.91	0.99
Head length	-	5.83	5.58	5.42
Hypodermic tube internal diameter	hd	0.570	0.330	0.185
Hypodermic tube length	hl	200	200	200
Plastic tube internal diameter	td	1.0	1.0	1.0
Plastic tube length	tl	1000	1000	1000

FIGURE 3: Measured midspan stator wake loss coefficient

FIGURE 4: Top: Formulation of side coefficients and possible angle functions. Bottom: Error estimate taken from quadrilateral diagonal length. Both from 2.67 mm probe

and $\pm 20°$ in pitch angle. At each yaw and pitch angle position the pressures on the five probe holes are recorded along with the stagnation and static pressures of the jet, measured using separate in-jet Pitot and static probes. The probe coefficients are then formulated as shown in Equations 1, and described in [15]. With this formulation of the calibration coefficients, the five-hole probe can be used to traverse in a non-nulling configuration by interpolating C_{total} and C_{static} from the measured values of C_{yaw} and C_{pitch}.

$$P_{mean} = \frac{1}{4}(P_{left} + P_{right} + P_{up} + P_{down})$$

$$C_{yaw} = \frac{P_{left} - P_{right}}{P_{centre} - P_{mean}}$$

$$C_{pitch} = \frac{P_{up} - P_{down}}{P_{centre} - P_{mean}} \tag{1}$$

$$C_{total} = \frac{P_o - P_{centre}}{P_{centre} - P_{mean}}$$

$$C_{static} = \frac{P_o - P}{P_{centre} - P_{mean}}$$

Probe Measurement Error

The three probes detailed in Table 1 are used to traverse the mid-span wake of a compressor stator in a rotating rig. The error incurred by each probe is quantified analytically with a new method. It is shown that the error increases with the probe head diameter.

The stator wake is traversed 0.25 chords downstream of the stator trailing edge. At this location the wake is approximately 7.1 mm thick. The probes traversing the wake have a relative size (D/w) of 0.38, 0.27 and 0.14. The traverse is made up of 107 points across the pitch, of which 51 points are hyperbolically clustered on the wake itself. This fine grid of traverse points is selected to ensure that errors do not arise from an inadequately resolved wake. The settling time for each probe is determined experimentally, in advance of the traverse, to be 3.7, 0.4 and 0.1 s for the 0.99, 1.91 and 2.67 mm probes respectively.

The results are post processed to include the single point spatial correction method detailed in [16] and [17]. This correction uses spacial interpolation to evaluate the side hole pressures as if they were in the same location as the centre hole. While it improves the accuracy of all of the probes it will be shown that it is unable to completely remove the error incurred from using a five-hole probe that is too large.

Figure 3 shows the stator blade wake measured with the three different sized five-hole probes. It can be seen that increasing probe size reduces the width and depth of the wake and this results
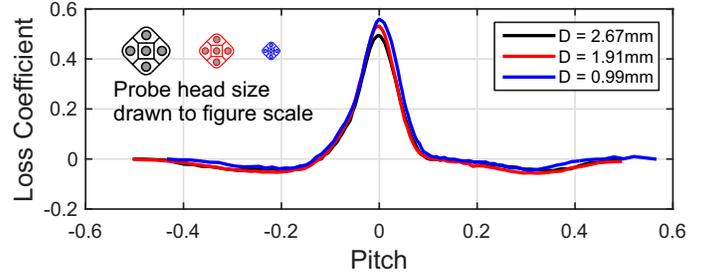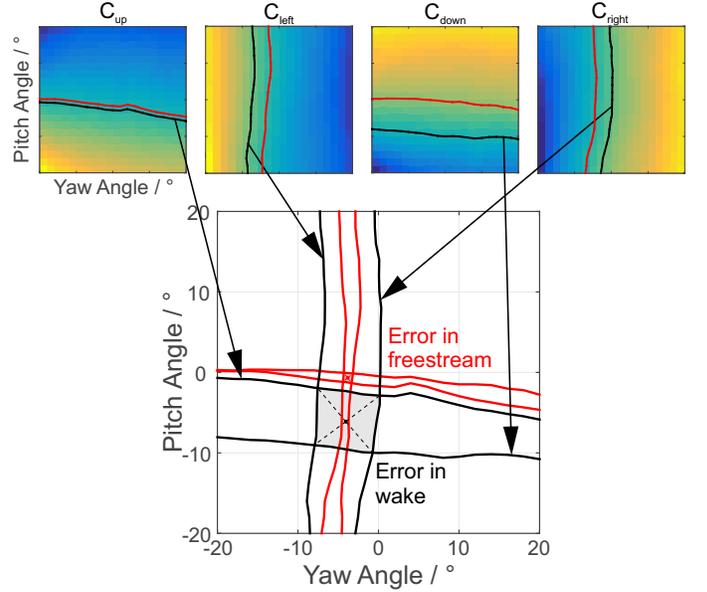
in a 35% reduction in mass-averaged loss coefficient. This type of measurement error could lead to an over prediction of blade performance and should be minimised by using small probes.

Five-hole probe errors can be quantified analytically by finding the distance a given measurement point lies from the "true" calibration plane. First, side hole coefficients for the top, bottom, left and right holes are calculated from the calibration data, according to Equation 2.

$$C_{side} = \frac{P_{side} - P_{centre}}{P_{centre} - P_{mean}} \tag{2}$$

The four side hole calibration coefficients vary across the space mapped out by the pitch and yaw angles. In the case of high and low yaw angles, the right and left side coefficients will reach a maximum and minimum. The top and bottom side coefficients will behave similarly for pitch. The variation of the side coefficients across the calibration plane is illustrated in the four contour plots shown in Fig. 4.

Next, for a given point in the traverse of a flow field, the side hole coefficients are re-calculated. These traverse measurement side hole coefficients correspond to a contour level on each of the four side hole calibration coefficients. The contour lines map out four functions that describe valid relationships between pitch and yaw angle based on the pressure coefficients measured. These functions
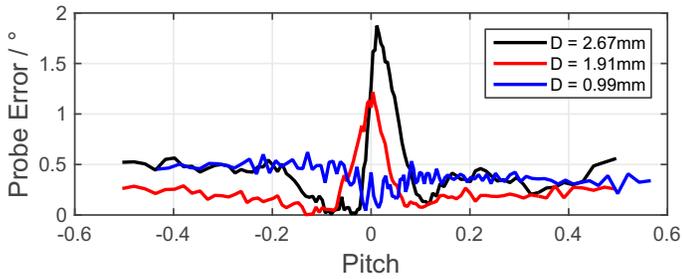
FIGURE 5: Calculated probe error in stator midspan wake

are plotted on top of the contour maps in Figure 4 for a measurement in the freestream (red) and in a wake (black).

In a case where there is no error, the four lines from each of the side coefficients intersect at a single point on the calibration plane. If the error is large, the intersection of the four lines describes a quadrilateral. The size of this quadrilateral is directly proportional to the error in the five-hole probe measurement. It quantifies how far away the measurement is from the true calibration plane.

The centre of the quadrilateral corresponds to the average pitch and yaw angles calculated using the coefficients specified in Equations 1. The probe error is quantified as the average distance between the centre point and each of the four corners of the quadrilateral. This quantity is an estimate of the angle error and is measured in degrees. The construction of the error quadrilateral and the diagonals is shown in the lower part of Fig. 4.

The error in traversing the stator wake is calculated for each of the three probes and is plotted in Fig. 5. As the probe passes through the shear layers in the stator wake the larger probes experience a greater error. In the case of the 0.99 mm probe the maximum error is 0.5° while the 2.67 mm probe has a maximum error of 1.9°.

The method described in this section is useful to researchers in three ways: first, it can determine if the five-hole probe is suitable for measuring a given flow field, second, it can be used to assess whether the probe needs recalibrating due to wear, and third, it can detect malfunctions such as blockage, leaks or rubs.

Trade Between Traverse Time and Accuracy

Area traverses are conducted over 2 stator passages and consist of 27 points across each pitch and 27 points from hub to casing. The points are clustered on the wakes and the end-wall boundary layers. The time taken to complete the 1458 traverse points is 2 hours and 5 minutes for the smallest probe and 36 minutes for the largest probe. The breakdown of time required to complete the various processes in these experiments is shown in Fig. 6. It can be seen that settling time dominates the run time in the case of the smallest probe. In the case of the biggest probe no time is wasted on settling the probe as the software used to conduct the traverse is able to perform other tasks during the specified delay period, such as logging instruments other than the pressure transducers.

It has been shown that selection of the probe diameter has two important and opposing consequences. First, in order to achieve high accuracy the probe diameter must be minimised. Second, in order to achieve short experimental run times the probe diameter should be increased. These results are summarised in Fig. 7 which shows the trade between measurement error and traverse time. For a given
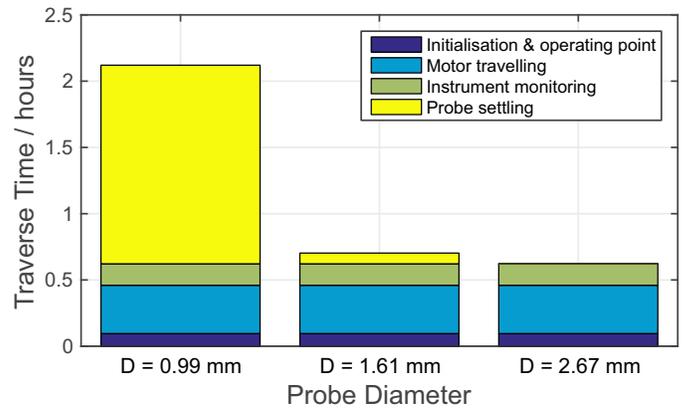

FIGURE 6: Breakdown of traverse times with different size probes
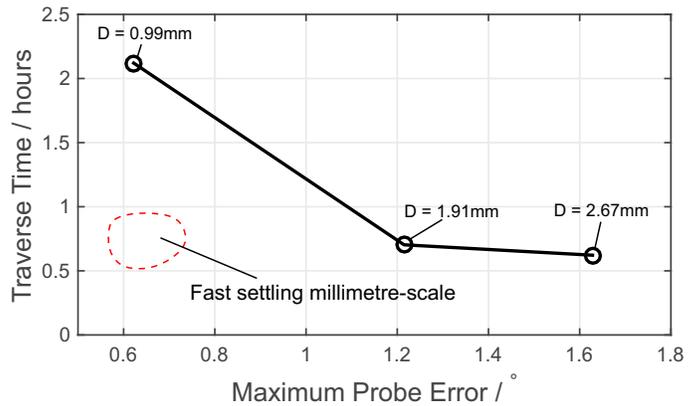

FIGURE 7: The trade between total traverse time and probe error

level of probe technology and for given constraints (length of probe, length of connecting tube), a curve similar to that shown in Fig. 7 sets the trade between accuracy and traverse time along which a designer can select a probe's size. In the second half of this paper the physical mechanisms that govern the increased settling time of smaller probes is investigated. This then aids in the design of small (<1 mm), fast-settling probes that beat the curve shown in Fig. 7.

2 ANALYTICAL MODEL FOR SETTLING TIME

The purpose of the analytical model is to predict the settling time of a five-hole probe given its internal geometry. The model is validated against experimental measurements using various lengths and diameters of hypodermic and plastic tube and it is shown that all cases relevant to mm-scale five-hole probe design are over-damped. Since the aim of the work is to predict settling time for steady flow measurements and the system is overdamped, the analytical model is validated with a step response.

This section describes the methodology used to develop the model and validates it against experimental measurements. It also shows the effect that different tube geometries have on settling time.

Methodology

The lumped parameter model described by Delio [8] represents a pressure sensing system as a tube with constant internal diameter
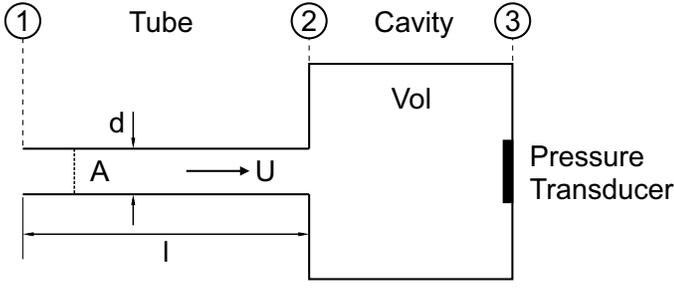
4

FIGURE 8: Tube connected to pressure transducer via a cavity

connected to a pressure transducer via a cavity, as shown in Fig. 8. For a five-hole probe, the tube in this system represents the smallest diameter hypodermic tube and the cavity represents the plastic tube and internal volume of the pressure transducer.

Delio [8] shows that the behaviour of the fluid in this system is represented by a second order differential equation:

$$\frac{\rho_{st} l}{A} \frac{Vol}{P_{st}} \frac{d^2 P_3}{dt^2} + \frac{32\mu l}{d^2 A} \frac{Vol}{\gamma P_{st}} \frac{dP_3}{dt} + P_3 = P_1 \qquad (3)$$

The numbered subscripts refer to the locations defined in Fig. 8 and subscript st refers to initial conditions. It is assumed that the change in pressure in the cavity is adiabatic and that the changes in pressure and density, compared to the initial values, are small. Equation 3 is in the standard form and the natural frequency and damping factor of the system are therefore defined as:

$$\omega_n = \sqrt{\frac{\gamma P_{st} A}{\rho_{st} l Vol}} \qquad (4)$$

$$\xi = \frac{16\mu}{d^2} \sqrt{\frac{l Vol}{\rho_{st} A \gamma P_{st}}} \qquad (5)$$

This well-established approach has two limitations when used to predict the settling time of five-hole probes. First, pressure drops due to friction in the plastic tube are not included and second it is not clear how "step-up" lengths of hypodermic tube diameter should be modelled. Bergh and Tijdeman [11] provide a complex approach which can model any number of tubes and cavities connected together in series. However, a simpler approach, which is still capable of modeling step-ups in tube diameter, is sought for this work.

In order to develop such a model it is useful to draw on the work of Taback [10] in which an analogy is made between the fluid system shown in Fig. 8 and a resistor, inductor capacitor circuit in series, where the output voltage is taken across the capacitor. The equation describing this circuit is identical in form to Equation 3. The geometry and fluid properties of the system in Fig. 8 can therefore be represented by an inductance, L, a resistance, R and a capacitance, C:

$$L = \frac{\rho l}{A} \qquad R = \frac{32\mu l}{d^2 A} \qquad C = \frac{Vol}{\gamma P_{st}} \qquad (6)$$

The electric circuit analogy is extended to model a tube and cavity system with step-ups in tube diameter. Figure 9 shows three tubes connected together and feeding into a cavity. This represents a probe made from two pieces of metal hypodermic tube attached to a pressure transducer via a length of plastic tube. The cavity now represents the internal volume of the pressure transducer. The
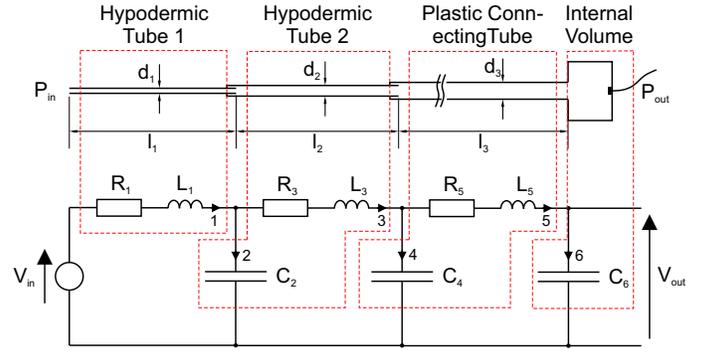

FIGURE 9: Probe with step-ups and analogous electric circuit

resistances, inductances and capacitances in each loop of the circuit are calculated with Equations 6 using the internal geometry of the associated tubes, as shown in Fig. 9.

The circuit in Fig. 9 is described by six first-order differential equations. These differential equations can be solved using an ordinary differential equation (ODE) solver, which typically requires less than 3 seconds to run on a laptop PC. This gives the output voltage, V_{out}, and hence by analogy, the pressure measured by the transducer.

The electric circuit analogy makes it easier to analyse the case where there are n step-ups in tube diameter. Using the same method, a generalised version of the electric circuit can be analysed and this results in a set of $2n$ first-order differential equations:

$$\begin{bmatrix} \frac{d\phi_1}{dt} \\ \frac{d\phi_3}{dt} \\ \vdots \\ \frac{d\phi_{2n-1}}{dt} \\ \frac{dq_2}{dt} \\ \frac{dq_4}{dt} \\ \vdots \\ \frac{dq_{2n}}{dt} \end{bmatrix} = B \begin{bmatrix} \frac{\phi_1}{L_1} \\ \frac{\phi_3}{L_3} \\ \vdots \\ \frac{\phi_{2n-1}}{L_{2n-1}} \\ \frac{q_2}{C_2} \\ \frac{q_4}{C_4} \\ \vdots \\ \frac{q_{2n}}{C_{2n}} \end{bmatrix} + \begin{bmatrix} V_{in} \\ 0 \\ \vdots \\ 0 \\ 0 \\ 0 \\ \vdots \\ 0 \end{bmatrix} \qquad (7)$$

$$B = \begin{bmatrix} \begin{bmatrix} R_1 & 0 & \dots & 0 \\ 0 & R_3 & \dots & 0 \\ \vdots & \vdots & \ddots & \vdots \\ 0 & 0 & \dots & R_{2n-1} \end{bmatrix} & \begin{bmatrix} -1 & 0 & \dots & 0 \\ 1 & -1 & \dots & 0 \\ \vdots & \ddots & \ddots & \vdots \\ 0 & \dots & 1 & -1 \end{bmatrix} \\ \begin{bmatrix} 1 & -1 & \dots & 0 \\ 0 & 1 & \ddots & 0 \\ \vdots & \vdots & \ddots & -1 \\ 0 & 0 & \dots & 1 \end{bmatrix} & \begin{bmatrix} 0 & 0 & \dots & 0 \\ 0 & 0 & \dots & 0 \\ \vdots & \vdots & \ddots & \vdots \\ 0 & 0 & \dots & 0 \end{bmatrix} \end{bmatrix} \qquad (8)$$

The output voltage, and hence pressure at the transducer, is given by:

$$V_{out} = \frac{q_{2n}}{C_{2n}} \qquad (9)$$

Experimental Methods

Experimental measurements were performed to validate the accuracy of the circuit analogy model, using the setup shown schematically in Fig. 10. This method is similar to that of Paniagua and Denos [18]. A balloon is mounted on a plug and burst close to its neck using a sharp point. The bursting balloon creates a step-change in pressure and this is measured by fast response pressure transducer (FRPT) 1 flush mounted in the plug. At the same time, FRPT 2 measures the pressure at the end of the test probe. The volume of the connecting piece between the plastic tube and FRPT 2 and the small cavity ahead of the pressure sensing membrane inside the transducer is 5×10^{-8} m^2. This is included in the analytical model and is called the pressure transducer internal volume.

The pressure transducers used are Kulite XCS-093 with a range of 35kPa and frequency response up to 100kHz. The pressure transducer signals are filtered at 20kHz and the amplified signals are digitized using a National Instruments data acquisition card with a sample rate of 100kHz.
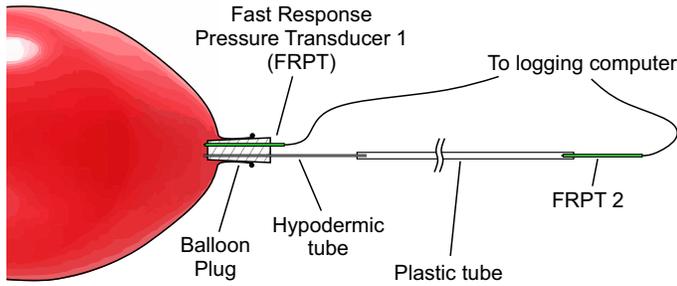

FIGURE 10: Experimental setup for measuring settling time of pneumatic probes

Table 2 shows the different probe geometries tested; these are grouped into three sets. The first set of 36 test cases is used to validate the overall applicability of the extended circuit analogy model for a range of tube geometries. The second set investigates the effect of step-ups in hypodermic tube diameter and the third set is used to study probes which use plastic tubing with small internal diameters (< 1.0 mm).

The settling time is defined as the time taken for the output response to match the step response to within a given error [19]. In this case the error is 1% of the step change in pressure.
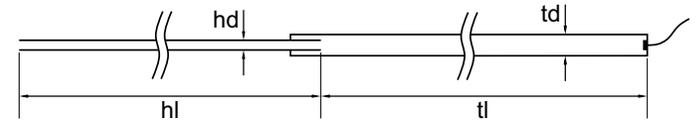
The internal diameters of the stainless steel hypodermic tubing used to construct the probes in this paper have a quoted variation of $\pm$ 15%. The settling time is particularly sensitive to the internal diameter of the tubing due to the d^2 term in the damping factor, ξ. Therefore the uncertainty in the internal geometry of the probe can lead to inaccurate settling time predictions.

Measuring an internal diameter of this size is not possible with standard linear measurement devices. In this paper the internal diameter is obtained indirectly by measuring the natural frequency of a cantilevered length of tubing. These tests can be performed with commonly available equipment and yield an accuracy of $\pm$ 0.01 mm ($\pm$ 5% for the smallest tube used).

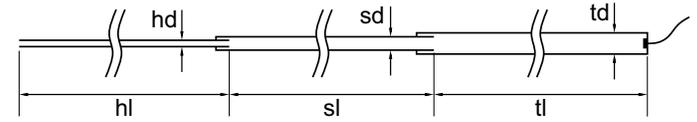The largest uncertainty in the cantilever frequency method is

TABLE 2: Test probe cases. All dimensions in mm
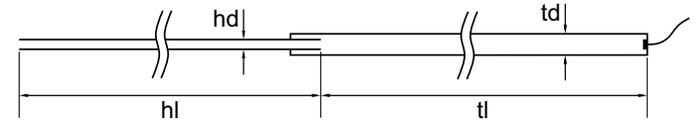
Set 1: Model validation

Hypodermic tube diameters	hd	0.185, 0.330, 0.570
Hypodermic tube lengths	hl	40, 100, 200
Plastic tube diameter	td	1.00
Plastic tube lengths	tl	100, 500, 1000, 3500

Set 2: Varying hypodermic tube step-up length

Narrow hypodermic tube diameter	hd	0.185
Narrow hypodermic tube lengths	hl	50, 100, 150, 200, 250
Step-up hypodermic tube diameter	sd	0.680
Step-up hypodermic tube lengths	sl	250, 200, 150, 100, 50
Plastic tube diameter	td	1.00
Plastic tube length	tl	3500

Set 3: Varying plastic tube internal diameter

Hypodermic tube diameter	hd	0.185
Hypodermic tube length	hl	200
Plastic tube diameters	td	0.185, 0.305, 0.40, 0.50 0.58, 0.75, 1.00
Plastic tube length	tl	1000

the Young's modulus; the tube manufacturer quotes values for 304 Stainless Steel from 193 GPa to 199 GPa. An optical microscope ($\times 40$ magnification) was also used to measure the internal diameter of the tubes, however, the resulting experimental uncertainty is greater than that of the cantilever frequency method. The uncertainty in measuring tube internal diameters is carried through into the model and the subsequent range of predicted settling times is calculated.

Results

In this section, the analytical model is used to study the effect on settling time of changes to the internal geometry of pneumatic probes. These results are also compared to experimental measurements in order to validate the model. The results are split into the three sets
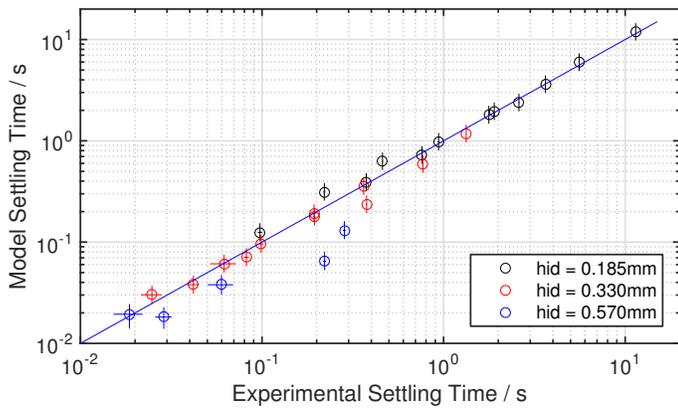
FIGURE 11: Comparison of measured and predicted settling times

FIGURE 12: Measured and predicted settling time against step-up length. hd = 0.185 mm, sd = 0.680 mm, td = 1.00 mm, tl = 3500 mm

FIGURE 13: Measured and predicted settling time against plastic tube internal diameter. hd=0.185 mm, hl=200 mm, tl=1000 mm

given in Table 2.

Set 1: Model Validation   Figure 11 shows the measured settling time plotted against the predicted settling time for the cases listed as Set 1 in Table 2. The tests were repeated and the standard deviations of the settling time tests are plotted as horizontal error bars. These are interpreted as a representation of the uncertainty in the measurements. Cases with measured settling times less than 0.01 s are not shown as the uncertainty is of the same order as the measurement itself. The vertical error bars show the range of settling times predicted by the model given the uncertainty in the internal diameter of the tubes.

All the cases plotted in Fig. 11 are over-damped. However, six cases with hypodermic tube internal diameter of 0.570 mm overshoot the step-response and are therefore under-damped. This is observed in the experimental measurements and predicted successfully by the analytical model. These cases are not shown in Fig. 11 since their settling time is less than 0.01 s. An under-damped probe could be designed with 0.570 mm hypodermic tube, however, for steady flow measurements this should be avoided as fluctuations in the flow could cause it to resonate. Also, 0.570 mm hypodermic tube has an outer diameter of 0.890 mm and is therefore too large to be used in mm-scale five-hole probes.

Figure 11 shows that the model predictions match the measurements well. For the hypodermic tubes with internal diameter of 0.185 mm and 0.330 mm the mean discrepancy between predictions and measurements is 12.7%. The model predictions for the third group of tubes, with internal diameter 0.570 mm, do not match the measurements as well as the other groups. The model under predicts the settling time compared to the measurements and the mean discrepancy is 31.6%.

Set 2: Varying Hypodermic Tube Step-up Length Figure 12 shows an excellent agreement between measured and predicted settling time against step-up length (i.e. the length of the 0.680 mm hypodermic tube). This demonstrates that the extended circuit analogy model is capable of predicting settling times for cases where there are step-ups in hypodermic tube diameter.

Figure 12 also shows that settling time is reduced from 17.80 s, with no step-up, to 3.14 s with a 250 mm step-up. This improvement occurs because reducing the length of the narrow hypodermic tube
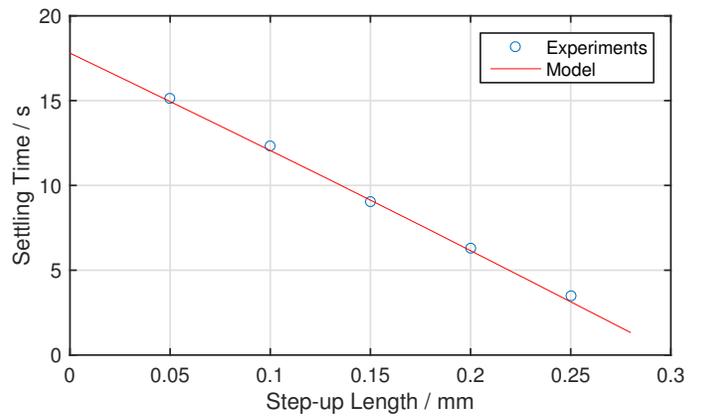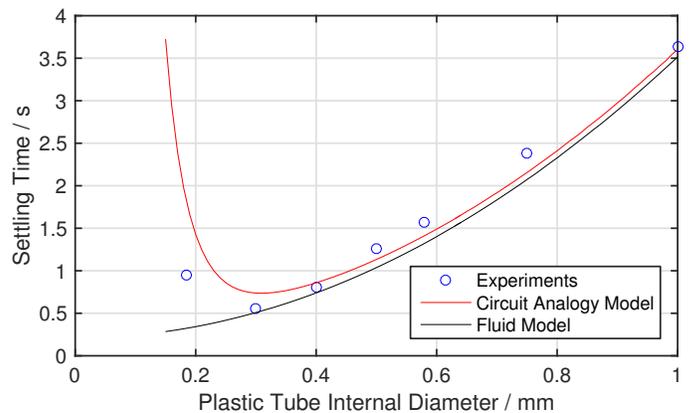
reduces the effect of friction. This has more influence on settling time than the small increase in volume (relative to the volume in the plastic tube) created by having a step-up.

Set 3: Varying Plastic Tube Internal Diameter Figure 13 shows settling time against plastic tube internal diameter from experimental measurements, the circuit analogy model and Delio's fluid model given in Equation 3. The measurements show that as the internal diameter of the plastic tube is reduced from 1.00 mm to 0.30 mm, the settling time reduces from 3.64 s to 0.55 s. However, for a tube with internal diameter 0.185 mm the settling time increases to 0.94 s. The minima occurs because there is a balance between the volume and effect of friction in the plastic connecting tube.

Figure 13 shows that the extended circuit analogy model matches the measurements well, including the minima and subsequent increase in settling time for internal diameters less than 0.30 mm. Delio's second order model only considers the volume of the plastic tube and not friction, so the minima is not captured and the settling time continues to fall as plastic tube diameter is reduced. This model, however, is in close agreement with the extended circuit analogy model for internal diameters greater than 0.40 mm, where the effect of friction in the plastic tube is negligible.

TABLE 3: Five-hole probe dimensions. All dimensions in mm

Probe		Datum	Optimised
Head diameter	D	0.99	0.99
Hypodermic tube diameter	hd	0.185	0.185
Hypodermic tube length	hl	200	100
Step-up tube diameter	sd	-	0.4
Step-up tube length	sl	-	100
Plastic tube diameter	td	1.0	0.4
Plastic tube length	tl	1000	200

3   OPTIMISED PROBE DESIGN

Probes with small outer dimensions (of order 1 mm) are required to achieve high accuracy when traversing flow fields in turbomachinery. The five-hole probe with outer diameter 0.99 mm, described in Table 1, gives the best accuracy out of those tested for this paper. However, this probe takes a long time to settle and a complete area traverse of two stator passages requires 2 hours and 6 minutes. This section presents a design with the same external geometry and therefore accuracy as the datum probe but with an optimised internal geometry that significantly reduces settling time.

The analytical model presented in Section 2 highlights three key areas where improvements can be made to the internal geometry:

First, the length of the plastic tubing that connects the rear of the probe to the bank of pressure transducers should be minimised. In this work it was possible to move the pressure transducers from a tower that contained racks of the experiment's instruments onto the traverse gear itself. The improved proximity of the pressure transducers to the rear of the probe enables the plastic tubing to be shortened from 1000 mm to 200 mm.

Second, the length of the smallest diameter of hypodermic tubing, which forms the head of the probe, should be minimised. This part of the probe is where friction restricts the velocity of the fluid, causing the rest of the probe to fill (pressurise) or evacuate (de-pressurise) slowly. In the optimised probe, the diameter is stepped-up after 100 mm to 0.4 mm. There is no issue fitting the step-up tubes into the stem of the probe, as can be seen in Fig. 2.

Finally, the diameter of the flexible plastic tubing should be reduced. It is necessary to select the diameter carefully, as a reduction past the optimum shown in Fig. 13 will have an adverse effect on the settling time. Plastic tubing with internal diameter of 0.4 mm is chosen as it is close to the optimum, is readily available and has good mechanical integrity.

The geometries of the original 0.99 mm probe and the optimised probe are compared in Table 3. The combination of the three improvements to the probe design reduces the settling time from 3.4 s to 0.29 s. The optimised probe is able to complete the area traverse described in Section 1 in 37 minutes, a reduction in time of 71%.

CONCLUSIONS

1. The selection of a five-hole probe's head diameter has a significant effect on both the accuracy that can be achieved in measuring a flowfield and the time required to complete an experiment. Small probes increase the accuracy of measurement, but delay the experiment by taking a longer time for pressure readings to settle between points.
2. The settling time is increased by small diameter hypodermic tubes and large volume connecting tubes. The small diameter tubes impose greater friction, this reduces the velocity and increases the time taken for the system to reach equilibrium. Large downstream volumes increase the time taken for settling as they take longer to equalise between readings.
3. In simple cases, where a single, small diameter hypodermic tube is connected to a pressure transducer via plastic tube, a second-order tube-cavity model is sufficient to predict the settling time accurately. This is because the plastic tube volume is large relative to the hypodermic tube volume, while the friction of the plastic tube is small relative to the hypodermic tube friction. Thus, the simple tube-cavity model matches reality well.
4. In more complex cases, where there are step-ups or small-diameter plastic connecting tube is used, a higher-order analytical model, using an extended electrical circuit analogy, is shown to predict the correct settling time. Overall, in 78% of cases tested it was possible to predict the settling time accurate to ± 10% of the measured value.
5. Use of the analytical model leads to probe designs with shorter connecting tubes with smaller internal diameter and step-up diameters within the probe itself. These design modifications maintain the accuracy of a 0.99 mm probe but reduces the settling time by 85%. In the example case it was therefore possible to reduce the traverse time from 2 hours 6 minutes down to 37 minutes.

NOMENCLATURE

A	Cross Sectional Area
C	Probe Coefficient or Electrical Capacitance
d	Tube Internal Diameter
D	Probe Head Diameter
l	Tube Length
L	Electrical Inductance
P	Pressure
P_0	Stagnation Pressure
q	Electrical Charge
R	Electrical Resistance
t	Time
V	Voltage
Vol	Cavity Volume
w	Wake Thickness
γ	Specific Heat Ratio
μ	Dynamic Viscosity
ξ	Damping Factor
ρ	Density of Gas

ϕ Electrical Flux

REFERENCES

[1] Ligrani, P., Singer, B., and Baun, L., 1989. "Miniature five-hole pressure probe for measurement of three mean velocity components in low-speed flows". *Journal of Physics E: Scientific Instruments,* **22**(10), p. 868.

[2] Lenherr, C., Kalfas, A., and Abhari, R., 2007. "A flow adaptive aerodynamic probe concept for turbomachinery". *Measurement Science and Technology,* **18**(8), p. 2599.

[3] Sieverding, C., Arts, T., Denos, R., and Brouckaert, J.-F., 2000. "Measurement techniques for unsteady flows in turbomachines". *Experiments in Fluids,* **28**(4), pp. 285–321.

[4] Ainsworth, R., Miller, R., Moss, R., and Thorpe, S., 2000. "Unsteady pressure measurement". *Measurement Science and Technology,* **11**(7), p. 1055.

[5] Naughton, J., Cattafesta, III, L., and Settles, G., 1993. "Miniature, fast-response five-hole conical probe for supersonic flowfield measurements". *AIAA journal,* **31**(3), pp. 453–458.

[6] Georgiou, D. P., and Milidonis, K. F., 2014. "Fabrication and calibration of a sub-miniature 5-hole probe with embedded pressure sensors for use in extremely confined and complex flow areas in turbomachinery research facilities". *Flow Measurement and Instrumentation,* **39**, pp. 54–63.

[7] Stecki, J., and Davis, D., 1986. "Fluid transmission lines - distributed parameter models part 1: A review of the state of the art". *Proceedings of the Institution of Mechanical Engineers, Part A: Journal of Power and Energy,* **200**(4), pp. 215–228.

[8] Delio, G. J., Schwent, G. V., and Cesaro, R. S., 1949. *Transient Behavior of Lumped-Constant Systems for Sensing Gas Pressures.* National Advisory Committee for Aeronautics.

[9] Iberall, A. S., 1950. *Attenuation of oscillatory pressures in instrument lines.* Defense Technical Information Center.

[10] Taback, I., 1949. *The response of pressure measuring systems to oscillating pressures.* National Advisory Committee for Aeronautics.

[11] Bergh, H., and Tijdeman, H., 1965. Theoretical and experimental results for the dynamic response of pressure measuring systems. Tech. rep., Nationaal Lucht-en Ruimtevaartlaboratorium.

[12] Gumley, S., 1983. "A detailed design method for pneumatic tubing systems". *Journal of Wind Engineering and Industrial Aerodynamics,* **13**(1), pp. 441–452.

[13] Holmes, J., and Lewis, R., 1987. "Optimization of dynamic-pressure-measurement systems. i. single point measurements". *Journal of Wind Engineering and Industrial Aerodynamics,* **25**(3), pp. 249–273.

[14] Whitmore, S. A., and Fox, B., 2009. "Improved accuracy, second-order response model for pressure sensing systems". *Journal of Aircraft,* **46**(2), pp. 491–500.

[15] Dominy, R., and Hodson, H., 1992. "An investigation of factors influencing the calibration of 5-hole probes for 3-d flow measurements". In ASME 1992 International Gas Turbine and Aeroengine Congress and Exposition, American Society of Mechanical Engineers, pp. V001T01A077–V001T01A077.

[16] Ligrani, P., Singer, B., and Baun, L., 1989. "Spatial resolution and downwash velocity corrections for multiple-hole pressure probes in complex flows". *Experiments in Fluids,* **7**(6), pp. 424–426.

[17] Chernoray, V., and Hjarne, J., 2008. "Improving the accuracy of multihole probe measurements in velocity gradients". In ASME Turbo Expo 2008: Power for Land, Sea, and Air, American Society of Mechanical Engineers, pp. 125–134.

[18] Paniagua, G., and Denos, R., 2002. "Digital compensation of pressure sensors in the time domain". *Experiments in fluids,* **32**(4), pp. 417–424.

[19] NASA, 2010. *Measuring and Test Equipment Specifications. NASA Measurement Quality Assurance Handbook ANNEX 2*, Vol. NASA-HDBK-8739.19-2. National Aeronautics and Space Administration.